NASA TECHNICAL MEMORANDUM

NASA TM X- 64625

REDUNDANCY MANAGEMENT OF ELECTROHYDRAULIC SERVOACTUATORS BY MATHEMATICAL MODEL REFERENCING

By Richard A. Campbell
Astrionics Laboratory

NASA

George C. Marshall Space Flight Center
Marshall Space Flight Center, Alabama

MSFC - Form 3190 (Rev June 1971)

TECHNICAL REPORT STANDARD TITLE PAGE

1. REPORT NO.	2. GOVERNMENT ACCESSION NO.	3. RECIPIENT'S CATALOG NO.
NASA TM X-64625		

4. TITLE AND SUBTITLE	5. REPORT DATE
Redundancy Management of Electrohydraulic Servoactuators by Mathematical Model Referencing	November 9, 1971
	6. PERFORMING ORGANIZATION CODE
7. AUTHOR(S)	8. PERFORMING ORGANIZATION REPORT #
Richard A. Campbell	
9. PERFORMING ORGANIZATION NAME AND ADDRESS	10. WORK UNIT NO.
George C. Marshall Space Flight Center Marshall Space Flight Center, Alabama 35812	11. CONTRACT OR GRANT NO.
	13. TYPE OF REPORT & PERIOD COVERED
12. SPONSORING AGENCY NAME AND ADDRESS	
National Aeronautics and Space Administration Washington, D. C. 20546	Technical Memorandum
	14. SPONSORING AGENCY CODE

15. SUPPLEMENTARY NOTES

Prepared by Astrionics Laboratory, Science and Engineering

16. ABSTRACT

A description of a mathematical model reference system is presented which provides redundancy management for an electrohydraulic servoactuator. The mathematical model includes a compensation network that calculates reference parameter perturbations induced by external disturbance forces. This is accomplished by using the measured pressure differential data taken from the physical system. This technique was experimentally verified by tests performed using the H-1 engine thrust vector control system for Saturn IB. The results of these tests are included in this report. It was concluded that this technique improves the tracking accuracy of the model reference system to the extent that redundancy management of electrohydraulic servosystems may be performed using this method.

17. KEY WORDS	18. DISTRIBUTION STATEMENT
Mathematical model referencing Redundancy management Electrohydraulic servoactuators Thrust vector control Aerodynamic surface control	Richard A Campbell STAR Announcement

19. SECURITY CLASSIF. (of this report)	20. SECURITY CLASSIF. (of this page)	21. NO. OF PAGES	22. PRICE
Unclassified	Unclassified	33	$3.00

MSFC - Form 3292 (May 1969)

TABLE OF CONTENTS

LISTS OF ILLUSTRATIONS

DEFINITION OF SYMBOLS

Symbol	Definition
A	Piston area
D	Viscous damping coefficient
K_c	Pressure feedback gain
K_{eq}	Equivalent system compliance
K_{fb}	Servoactuator position feedback gain
K_s	Compliance of vehicle structure
K_v	Servovalve flow gain
M	Engine mass
S	Laplace operator
X_c	Position command signal
X_1	Position of physical system
X_2	Position of mathematical model
β_a	Position of servoactuator piston
$\overline{\beta}_a$	Corrected calculated position of servoactuator piston
β_{ac}	Calculated position of servoactuator piston
β_{am}	Measured position of servoactuator piston
β_c	Position command signal

DEFINITION OF SYMBOLS (Concluded)

Symbol	Definition
β_e	Position of engine
$\overline{\beta}_e$	Corrected calculated position of engine
β_{ec}	Calculated position of engine
β_{em}	Measured position of engine
β_l	Position of servoactuator load
$\overline{\beta}_l$	Corrected calculated position of servoactuator load
β_{lc}	Calculated position of servoactuator load
β_{ld}	Load position perturbations caused by extreme disturbance forces
β_{lm}	Measured position of servoactuator load
Δx	Position tracking error
ζ	Damping ratio
τ_f	Time constant in the pressure feedback compensation
ϕ	Phase angle associated with mathematical model response
ψ	Phase angle associated with physical system response
ω	Natural frequency

TECHNICAL MEMORANDUM X- 64625

REDUNDANCY MANAGEMENT OF ELECTROHYDRAULIC SERVOACTUATORS BY MATHEMATICAL MODEL REFERENCING

INTRODUCTION

As the size and complexity of space vehicles and aircraft are increasing, more and more emphasis is being placed on safety. This emphasis is being reflected in the design of electrohydraulic control systems by the use of both highly reliable components and redundant systems.

Redundancy in electrohydraulic control systems is accomplished by either the force-sharing or the detection-correction method. Force-sharing or, more precisely, force-summing is accomplished by the simultaneous use of parallel control units. The summation of control forces may occur either within the actuator or directly on the load. The simplicity and directness of this method accounts for its prevalence today. The detection-correction method, unlike force-sharing, operates with series elements. Redundancy is developed by removing any failed component from the system and replacing it with a standby. A system malfunction is detected by comparing pertinent parameters of the operational system with those of a reference system. The reference system's parameters may be generated by various methods, one of which is the use of a mathematical model of the system. The operational system is assumed to be operating correctly when the differences between the compared parameters remain below some set limit.

REDUNDANCY BY MATHEMATICAL MODELING

An example of a fail/operate redundant electrohydraulic servosystem which employs the mathematical modeling technique is shown in Figure 1.

The actuator's load position command β_c is applied simultaneously to both the computerized model and the physical system. The reference parameter used in this example is the load's position β_l; other parameters that could have been used are the actuator's position or the servovalve's spool position.

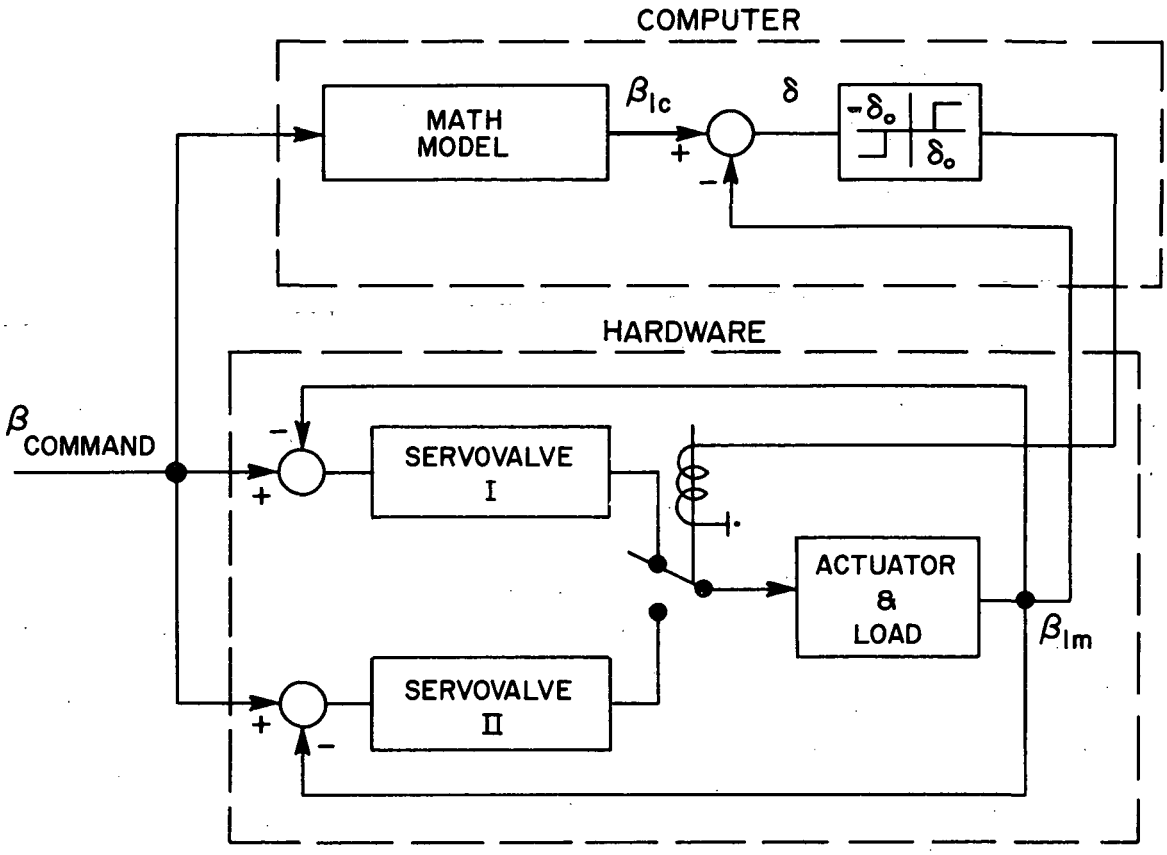

Figure 1. Fail/operate electrohydraulic servosystem.

When the difference between the measured load position β_{lm} (t) and the calculated load position β_{lc} (t) exceeds the allowable error $\pm\delta_0$ set in the comparator, the system is assumed to have sustained a failure. The output signal from the comparator then energizes the necessary corrective device such as a solenoid, which removes the failed component and replaces it with a standby.

The magnitude of an allowable error is determined from the dynamic performance tolerance placed on that particular control system. The computational electronics that comprise the error detection system must be capable of providing transient data of the reference parameter with sufficient accuracy to enable detection of a failure when the performance tolerances of that system are exceeded. For low-performance systems, a simple RC lag circuit may be sufficient, whereas more sophisticated systems may require models consisting of several operational amplifiers.

The method just described works very well for systems that do not encounter external disturbance forces. However, for systems that do, such as air-surface controllers and thrust-vector controllers, the above method can produce the erroneous conclusion that a component has failed since the tracking error may exceed the set threshold limits of the comparator during the time the external force is applied.

LOAD COMPENSATION

One method of correcting this problem would be to increase the threshold limits placed on the comparator. This, however, would decrease the sensitivity of the system to detect malfunctions as well as increase the time required for correction. Another means is to modify the calculated reference parameter so that it reflects the perturbations of the physical system. Theoretically, this can be accomplished if one knows the magnitude and direction of the disturbance force. This information can be obtained from the pressure differential measurement made across the actuator's piston.

The measured pressure differential has two components: that which results from command signals and that which is produced by an external disturbance force:

$$\Delta P_{measured} = \Delta P_{command} - \Delta P_{disturbance} . \quad (1)$$

Since the mathematical model can easily be programed to yield the pressure differential developed by the command, the ΔP induced into the system by the disturbance force can be obtained by subtracting ΔP command from ΔP measured:

$$\Delta P_{disturbance} = \Delta P_{measured} - \Delta P_{command} . \quad (2)$$

Knowing the dynamics of the control system, one can derive the transfer function which relates the disturbance force to the induced pressure differential in the actuator. This can be written in a general form as

$$\frac{\Delta P_{disturbance}}{F_{disturbance}} = \frac{A(S)}{B(S)} . \quad (3)$$

A second transfer function that relates the load's position perturbations caused by external disturbance forces must also be derived. It can be written as

$$\frac{\beta_{ld}}{F_{disturbance}} = \frac{D(S)}{B(S)} \quad . \tag{4}$$

From these two transfer functions, one can obtain the compensation network, K(S), which, when multiplied by $\Delta P_{disturbance}$, will generate the load's position perturbations. This network is obtained by dividing equation (4) by equation (3), yielding

$$\frac{\beta_{ld}}{\Delta P_{disturbance}} = \frac{D(S)}{A(S)} = K(S) \quad , \tag{5a}$$

or

$$\beta_{ld} = K(S)\ \Delta P_{disturbance} \tag{5b}$$

where $\Delta P_{disturbance}$ was calculated as indicated by equation (2). Adding these perturbations to the calculated load position, one obtains a new and more accurate value of the load position $\overline{\beta}_l$, which can now be used as the new reference parameter.

$$\overline{\beta}_l(t) = \beta_{lc}(t) + \beta_{ld}(t) \quad . \tag{6}$$

A schematic of a fail/operate system using this external force compensation technique is shown in Figure 2.

CONCEPT VERIFICATION TESTING

A test program was devised to verify the disturbance load compensation concept and to establish a criterion for the magnitude of tracking accuracy which the mathematical model could produce when measured with respect to a physical system. A Saturn IB H-1 engine thrust vector control system was used for these tests. An illustration of the test configuration and the location where test data were recorded are shown in Figure 3. The measured parameters were:

β_{am} - Position of the servoactuator piston rod, measured with respect to the servoactuator housing.

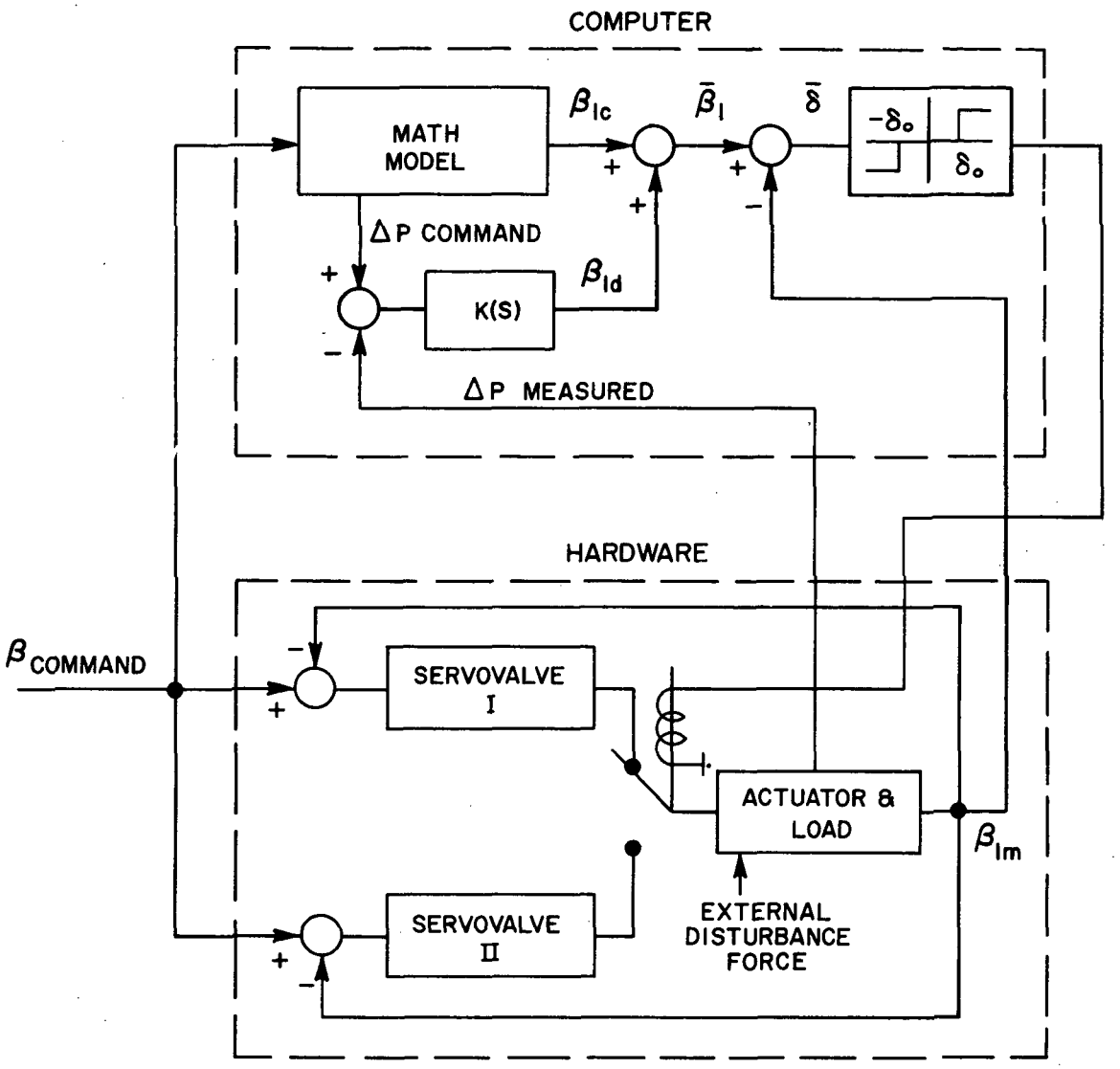

Figure 2. Fail/operate electrohydraulic servosystem with external load compensation.

β_{em} - Position of the engine measured with respect to the frame of the engine simulator.

ΔP_m - Pressure differential measured across the servoactuator piston.

A block diagram of the mathematical model as it was programed on the analog computer is shown in Figure 4. The assumptions and derivations of equations used to generate Figure 4 are presented in the Appendix. The symbols used in the block diagram are listed in this report in the Definition of Symbols.

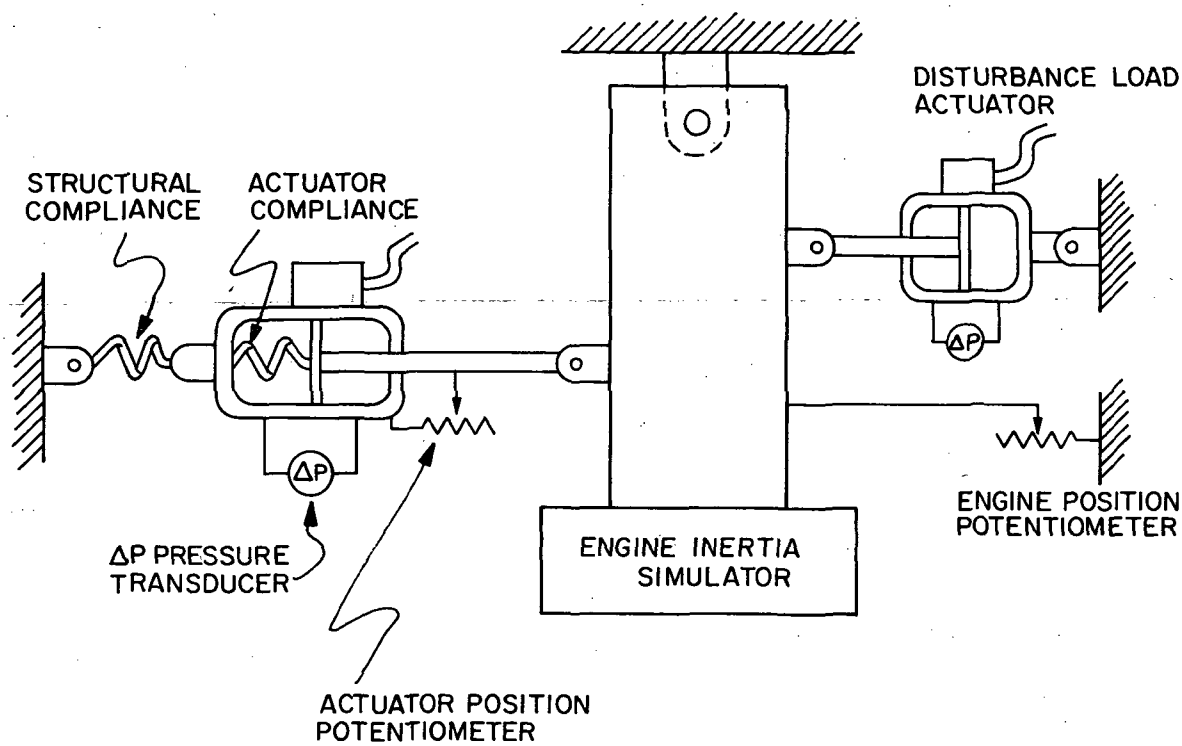

Figure 3. System hardware simulation.

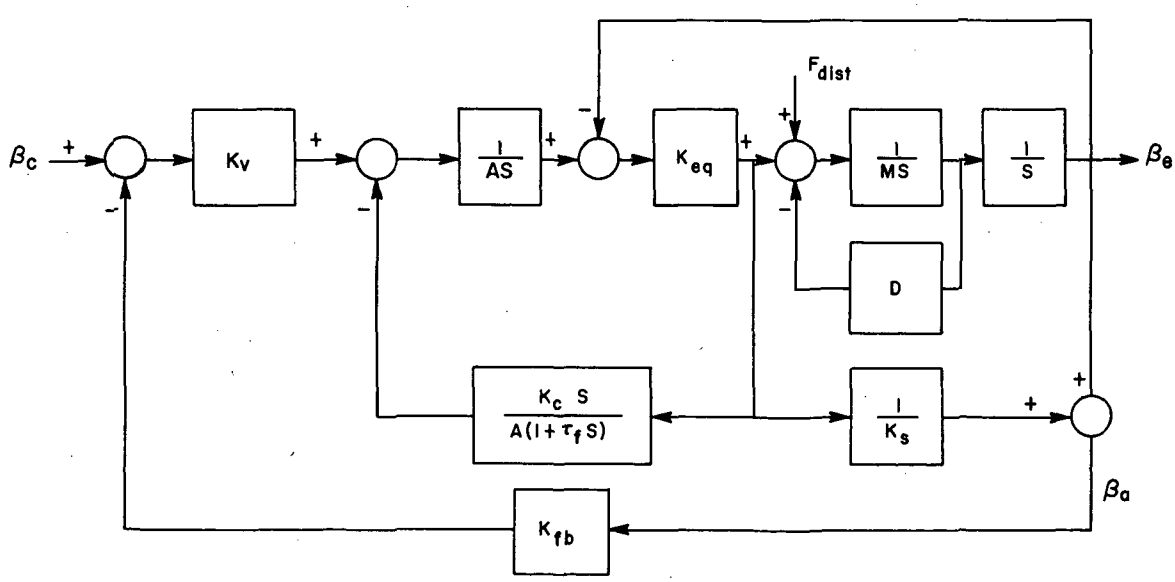

Figure 4. H-1 engine thrust vector control system.

The first test was performed to determine the computational accuracy of the mathematical model for both engine position commands and external disturbance forces. This was accomplished by developing tracking errors for various system parameters. These error signals were generated by subtracting the computed value from its measured counterpart on the physical system. Tracking errors were generated for the following system parameters: engine position β_e, actuator position β_a, and actuator pressure differential ΔP. These errors can be expressed mathematically as:

$$\delta\beta_e = \beta_{em} - \beta_{ec} \quad . \tag{7}$$

$$\delta\beta_a = \beta_{am} - \beta_{ac} \quad . \tag{8}$$

$$\delta\Delta P = \Delta P_m - \Delta P_c \quad . \tag{9}$$

The results of the test for 1/2 deg and 1 deg commands are shown in Figures 5 and 6, respectively. The maximum recorded errors were

Command (deg)	$\delta\beta_a$ (deg)	$\delta\beta_e$ (deg)	$\delta\Delta P$ (N/cm^2)
Step 1/2	0.08	0.1	19.30
Step 1	0.16	0.2	35.84

Next, step disturbance loads of ±8896 N (±2000 lb) were applied to the engine, while the servoactuator was being commanded to hold zero position. The data recorded during this test are shown in Figure 7. The following maximum tracking errors were measured:

Disturbance Loads	$\delta\beta_a$	$\delta\beta_e$
Step ±8896 N (±2000 lb)	0.35 deg	0.46 deg

The tracking errors determined during these tests will serve as a baseline for comparison in the evaluation of the load compensation technique.

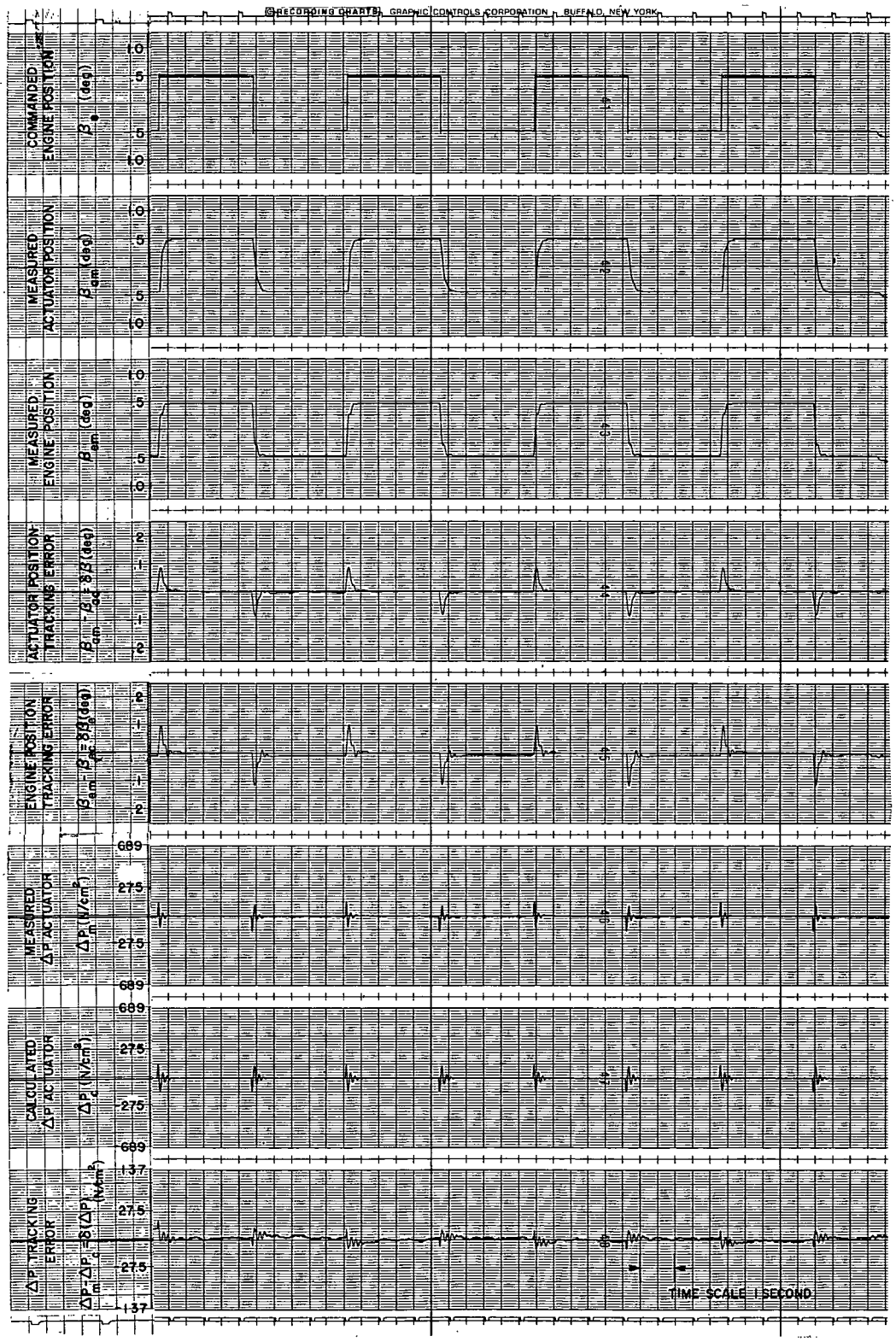

Figure 5. One-half-degree step command with uncompensated reference system.

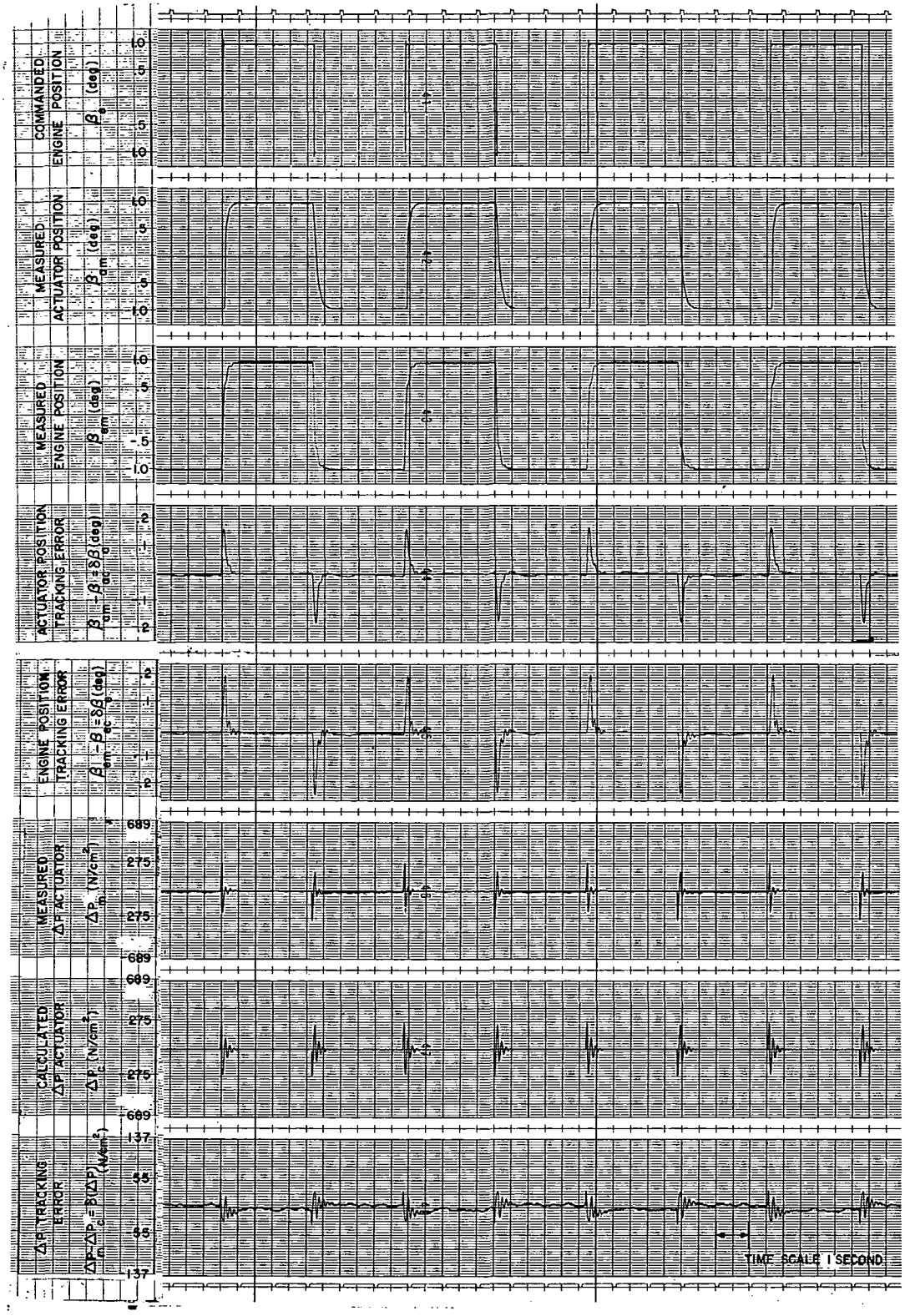

Figure 6. One-degree step command with uncompensated reference system.

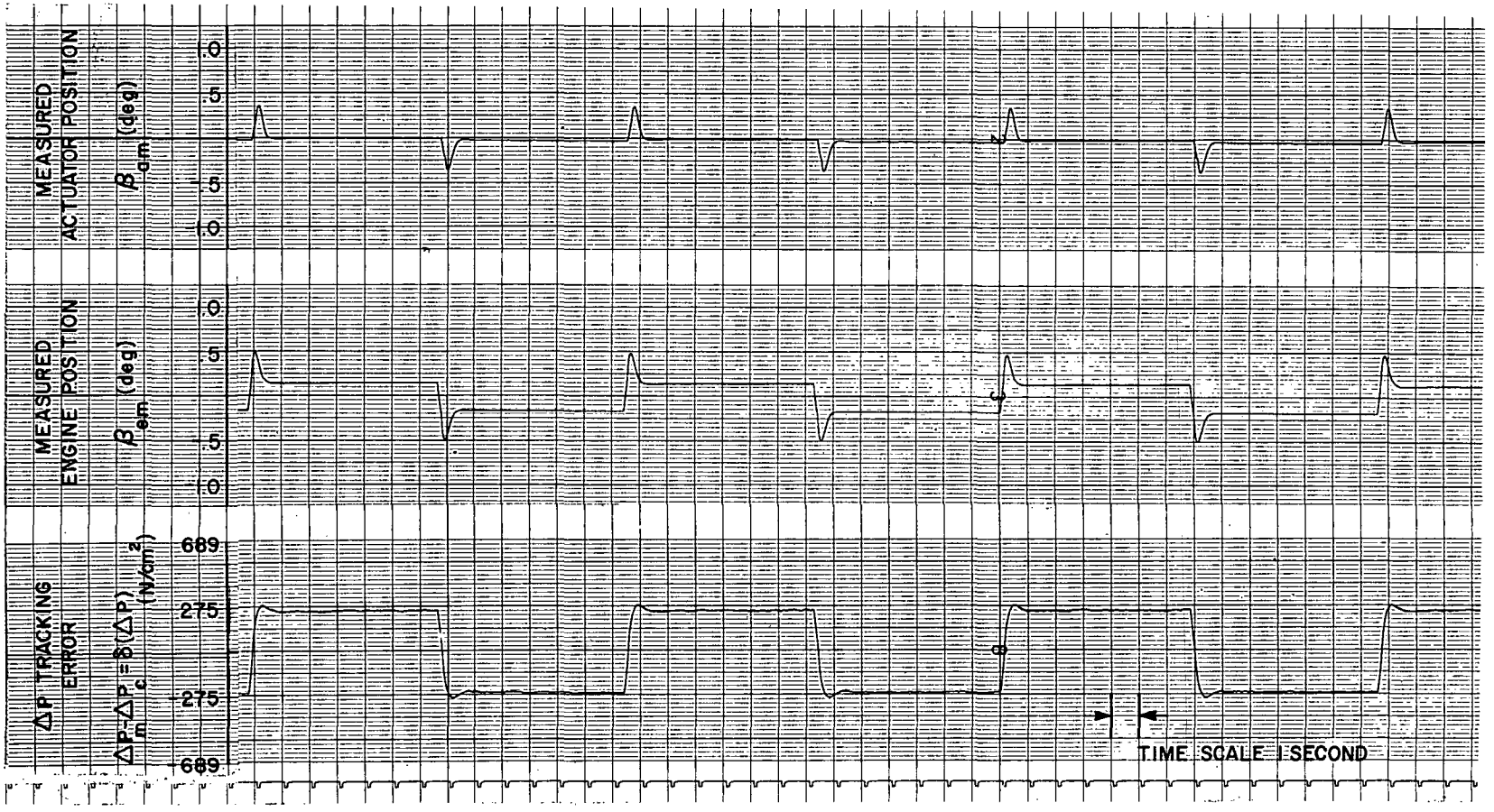

Figure 7. 8896-N step disturbance force with uncompensated reference system.

COMPENSATION NETWORK TESTS

The mathematical model was then changed to include compensation networks for both the engine and actuator position reference parameters. The transfer functions that relate each of the chosen reference parameters to the disturbance force are given as

$$\frac{\beta_a(S)}{F_{disturbance}(S)} = \frac{A^2\tau_f(K_s - K_{eq})S^2 + \left[K_{eq}K_sK_c + A^2(K_s - K_{eq})\right]S}{D(S)} \tag{10}$$

and

$$\frac{\beta_e(S)}{F_{disturbance}} = \frac{A^2K_s\tau_fS^2 + (K_sK_{eq}K_c + K_{eq}K_vK_{fb}A\tau_f + A^2K_s)S + K_{eq}K_vK_{fb}A}{D(S)}, \tag{11}$$

where the denominator D(S) is the system characteristic equation which is given by

$$\begin{aligned} D(S) = {} & MA^2K_s\tau_fS^4 + \left[A^2K_s(M + D\tau_f) + AK_vK_{fb}K_{eq}M\tau_f + MK_{eq}K_sK_c\right]S^3 \\ & + \left[A^2K_sD + AK_vK_{fb}K_{eq}(M + D\tau_f) + DK_{eq}K_sK_c + A^2K_{eq}K_s\tau_f\right]S^2 \\ & + \left[AK_{fb}K_vK_{eq}K_s\tau_f + AK_vK_{fb}K_{eq}D + A^2K_{eq}K_s\right]S \\ & + AK_{fb}K_vK_{eq}K_s \end{aligned} \tag{12}$$

These transfer functions were derived from the block diagram shown in Figure 4. The other transfer function required for calculating the compensation network is

$$\frac{\Delta P_m(S)}{F_{disturbance}(S)} = \frac{-K_{eq}K_s\left[A\tau_fS^2 + \left(K_vK_{fb}\tau_f + A\right)S + K_vK_{fb}\right]}{D(S)}, \tag{13}$$

which was also derived from Figure 4.

Since two reference parameters were being generated for this test, two load compensation networks were necessary. The network required to yield the engine position perturbations is obtained by dividing equation (11) by equation (13), yielding

$$K_e(S) = \frac{A^2 K_s \tau_f S^2 + \left(K_s K_{eq} K_c + K_{eq} K_v K_{fb} A \tau_f + A^2 K_s\right) S + K_{eq} K_v K_{fb} A}{K_{eq} K_s \left[A \tau_f S^2 + \left(K_v K_{fb} \tau_f + A\right) S + K_v K_{fb}\right]} . \quad (14)$$

The compensation network for actuator perturbation is obtained by dividing equation (10) by equation (13), yielding

$$K_a(S) = \frac{A^2 \tau_f \left(K_s - K_{eq}\right) S^2 + \left[K_{eq} K_s K_c + A^2 \left(K_s - K_{eq}\right)\right] S}{K_{eq} K_s \left[A \tau_f S^2 + \left(K_v K_{fb} \tau_f + A\right) S + K_v K_{fb}\right]} . \quad (15)$$

A block diagram of the mathematical model that was programed on the AD-64 analog computer and used for the test is shown in Figure 8. This test, like the first, was divided into two parts. The first was performed to establish the tracking errors when no disturbance forces were present. The measured tracking errors for a 1-deg step command were

Command	$\delta \overline{\beta}_a$	$\delta \overline{\beta}_e$
Step 1 deg	0.17 deg	0.29 deg

as shown on the recorded test data in Figure 9.

Both of these errors are greater than those recorded when using the uncompensated model. This is caused by a difference which exists between the measured pressure differential and the calculated pressure differential, even though no external loads were present. Thus, the tracking error in the ΔP parameter (shown on trace 8 of Figure 9) makes it appear to the model as if a disturbance load were present and thus produces an additional displacement in both actuator and engine positions.

For the second half of the test, a disturbance force was again applied, and the tracking errors were measured. The maximum recorded errors were

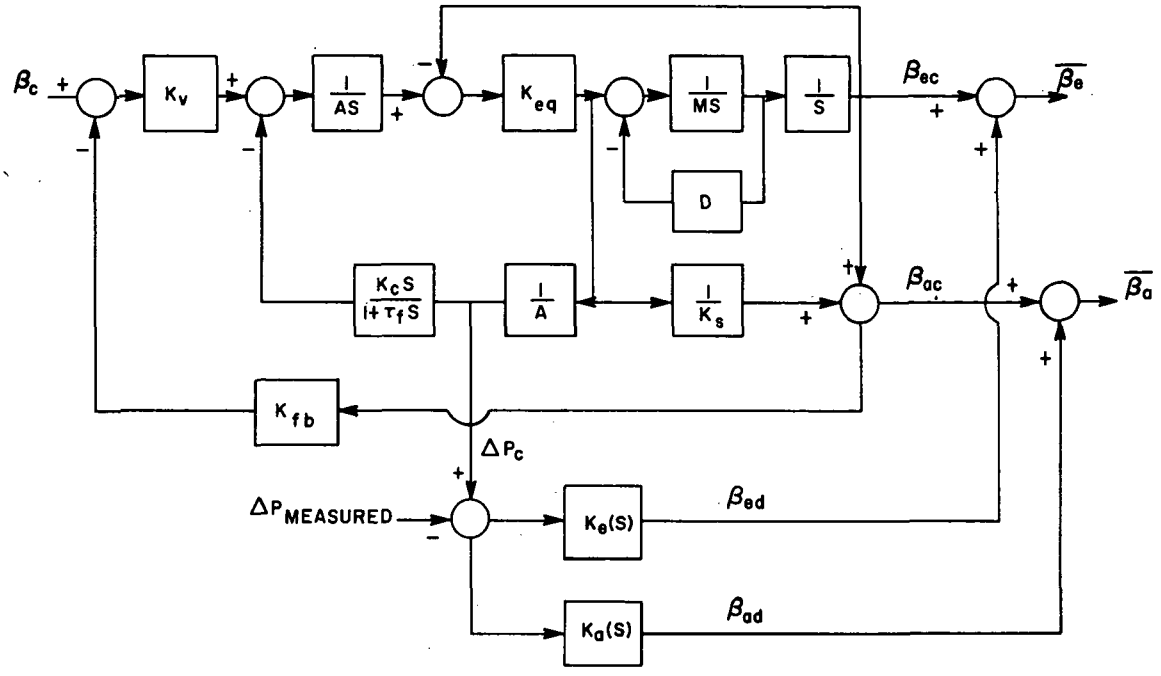

Figure 8. H-1 engine thrust vector control system including the external force compensation.

Disturbance Force	$\delta\overline{\beta}_a$	$\delta\overline{\beta}_e$
Step 8896 N(2000 lb)	0.10 deg	0.40 deg

as shown in Figure 10. The magnitude of these errors indicates that a substantial improvement in the system tracking accuracy can be obtained with the addition of the load compensation network. The actuator tracking accuracy was improved by a factor of 3.5.

TRACKING ERROR SENSITIVITY

A point of academic interest is the sensitivity of the tracking errors to variations in system parameters. To illustrate these effects, the damping ratio and natural frequency will be varied on a simple second-order system. Let the transfer function for the physical system be given as

$$\frac{X_1(S)}{X_c(S)} = \frac{\omega_1^2}{S^2 + 2\zeta_1\omega_1 S + \omega_1^2} \quad , \tag{16}$$

where the subscript 1 denotes a physical system parameter.

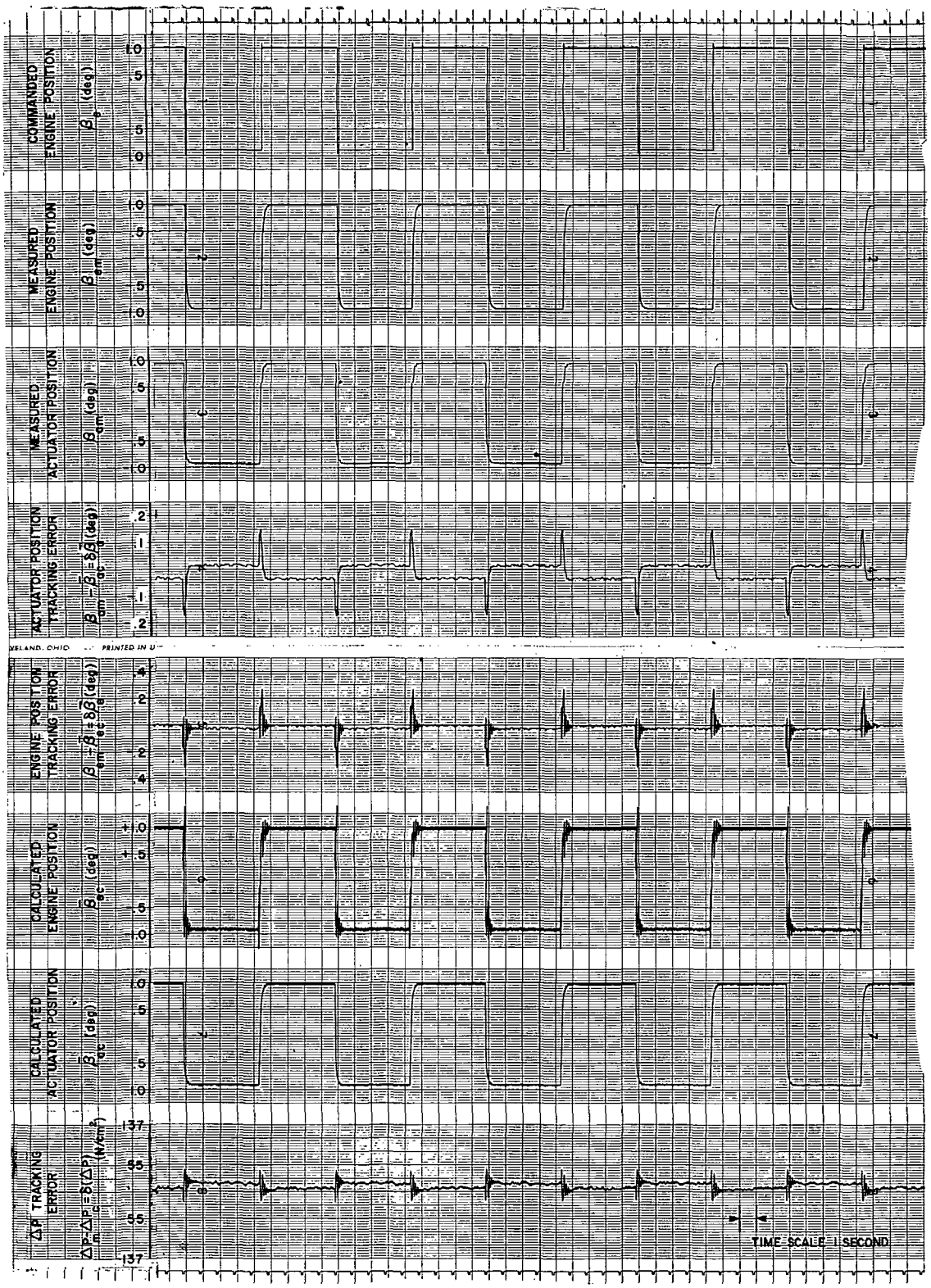

Figure 9. One-degree step command with compensated reference system.

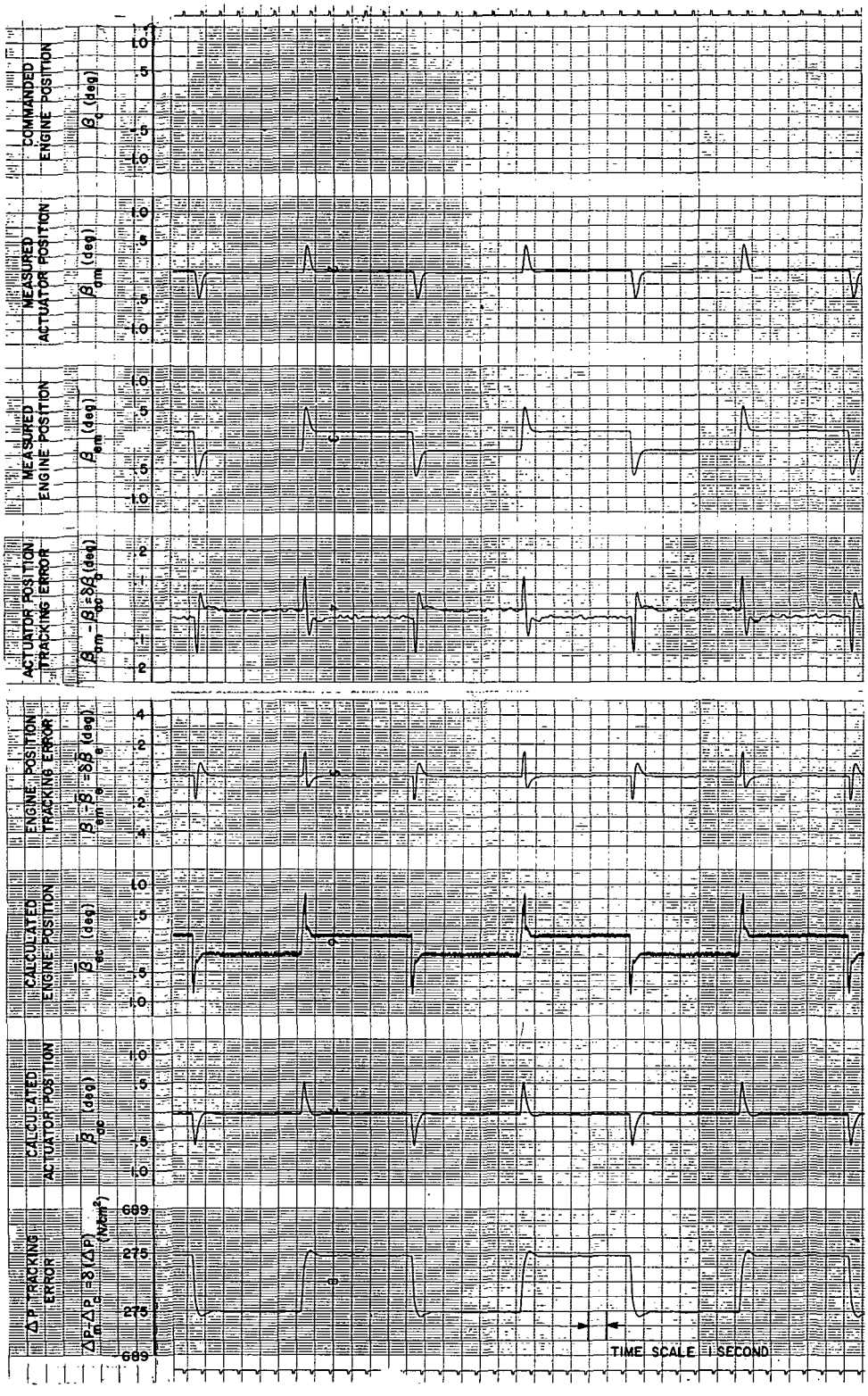

Figure 10. 8896-N step disturbance force with compensated reference system.

The transfer function used in the mathematical model is

$$\frac{X_2(S)}{X_c(S)} = \frac{\omega_2^2}{S^2 + 2\zeta_2\omega_2 S + \omega_2^2} \quad . \tag{17}$$

The mathematical model parameters, denoted by the subscript 2, are considered constant and programed into the model at their nominal system values. The tracking error Δx is then generated as shown in Figure 11.

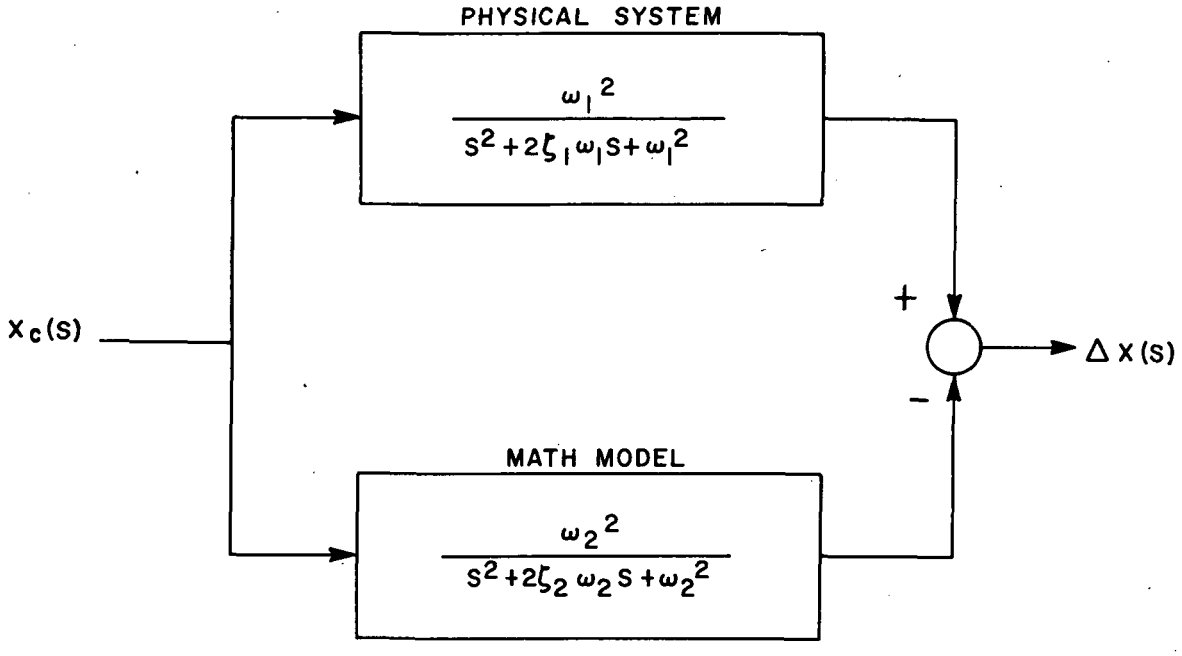

Figure 11. Tracking error sensitivity model reference system.

A general expression describing the error resulting from a unit step command is

$$\Delta x(S) = \left(\frac{\omega_1^2}{S^2 + 2\zeta_1\omega_1 S + \omega_1^2} - \frac{\omega_2^2}{S^2 + 2\zeta_2\omega_2 S + \omega_2^2} \right) \frac{1}{S} \quad , \tag{18}$$

or, written in the time domain,

$$\Delta x(t) = \frac{e^{-\zeta_1\omega_1 t}}{\sqrt{1-\zeta_1^2}} \sin\left(\omega_1\sqrt{1-\zeta_1^2}\, t - \psi\right) - \frac{e^{-\zeta_2\omega_2 t}}{\sqrt{1-\zeta_2^2}} \sin\left(\omega_2\sqrt{1-\zeta_2^2}\, t - \phi\right) . \tag{19}$$

The phase angles ψ and ϕ are

$$\psi = \tan^{-1} \frac{\sqrt{1 - \zeta_1^2}}{-\zeta_1}$$

$$\phi = \tan^{-1} \frac{\sqrt{1 - \zeta_2^2}}{-\zeta_2} \quad .$$

The effects of variations in ζ_1 and ω_1 were investigated by plotting equation (19) versus time. The first set of curves, shown in Figure 12, illustrates the effects of varying the system damping ratio (ζ_1) while holding all other parameters constant.

$$\omega_1 = \omega_2 = 6.00 \text{ Hz}$$

$$\zeta_2 = 0.707 \quad .$$

A second set of curves, shown in Figure 13, was plotted for variations in the system's natural frequency (ω_1). Again, all the other parameters were held constant.

$$\omega_2 = 6.00 \text{ Hz}$$

$$\zeta_1 = \zeta_2 = 0.707 \quad .$$

The most obvious difference between the two sets of curves is the time variation associated with the maximum tracking error when the system's natural frequency is the variable.

A better perspective of the effects of these parameter variations can be seen when one plots the data shown in Figures 12 and 13 in the form of maximum tracking error versus percentage of change in parameter. Where the percentage in parameter is given by

$$\text{percentage change} = \frac{\text{system value - model value}}{\text{system valve}} (\times 100) \quad , \tag{20}$$

the results are shown in Figure 14. This curve clearly illustrates that variations in the system's natural frequency will produce greater tracking errors than the same variations in the system damping ratio.

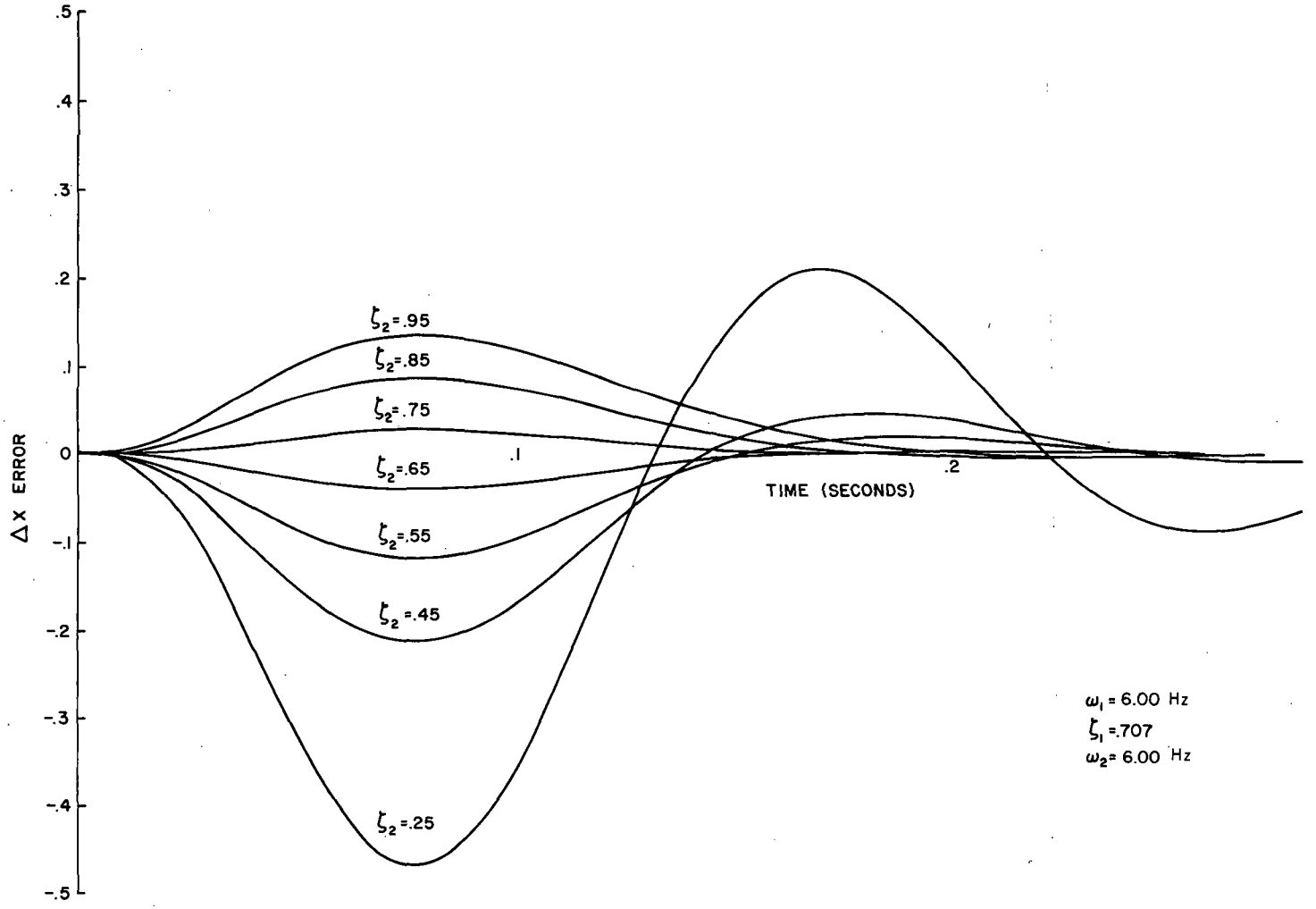

Figure 12. Normalized tracking error vs time for second-order system with ζ_2 as the variable parameter.

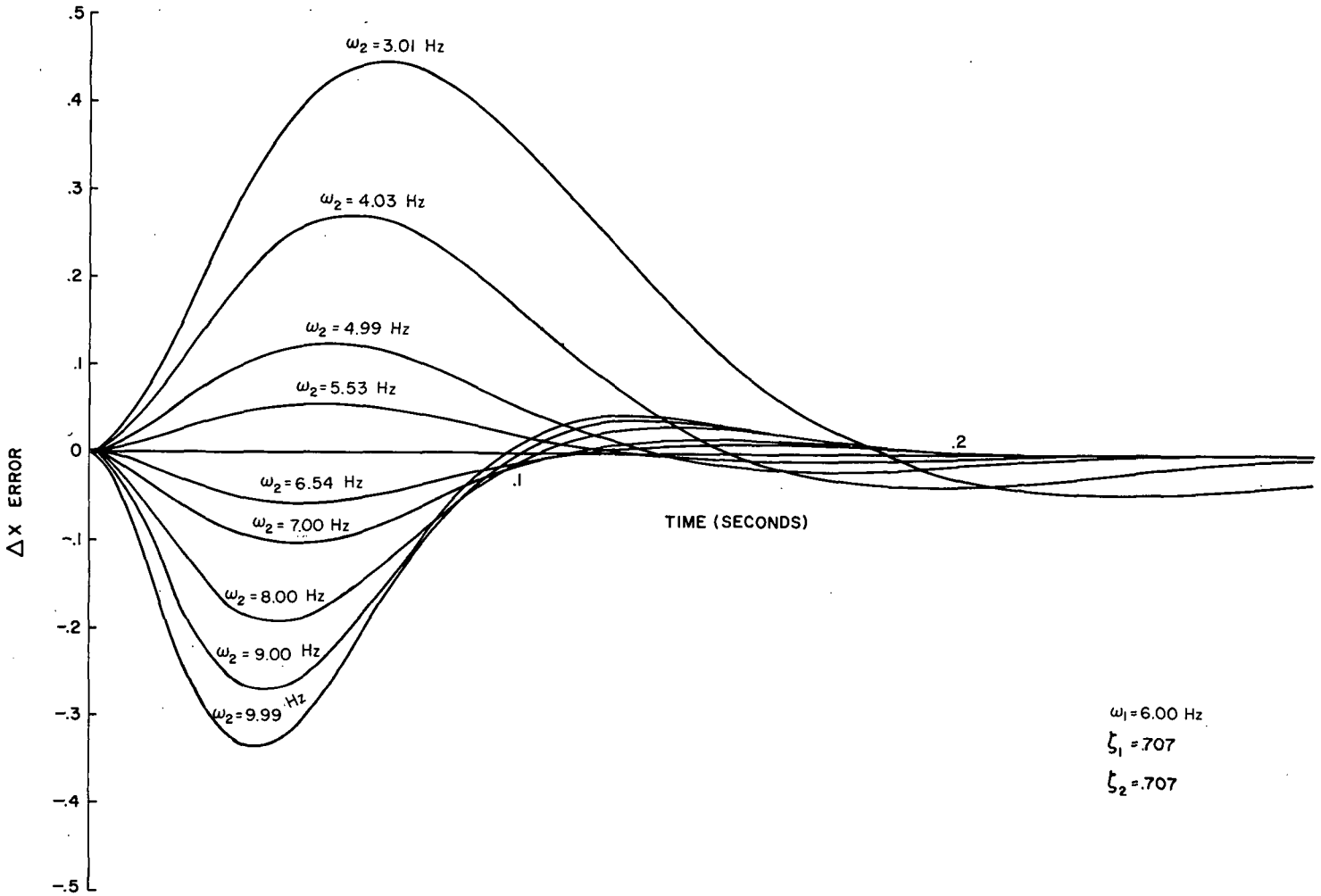

Figure 13. Normalized tracking error vs time for second-order system with ω_2 as the variable parameter.

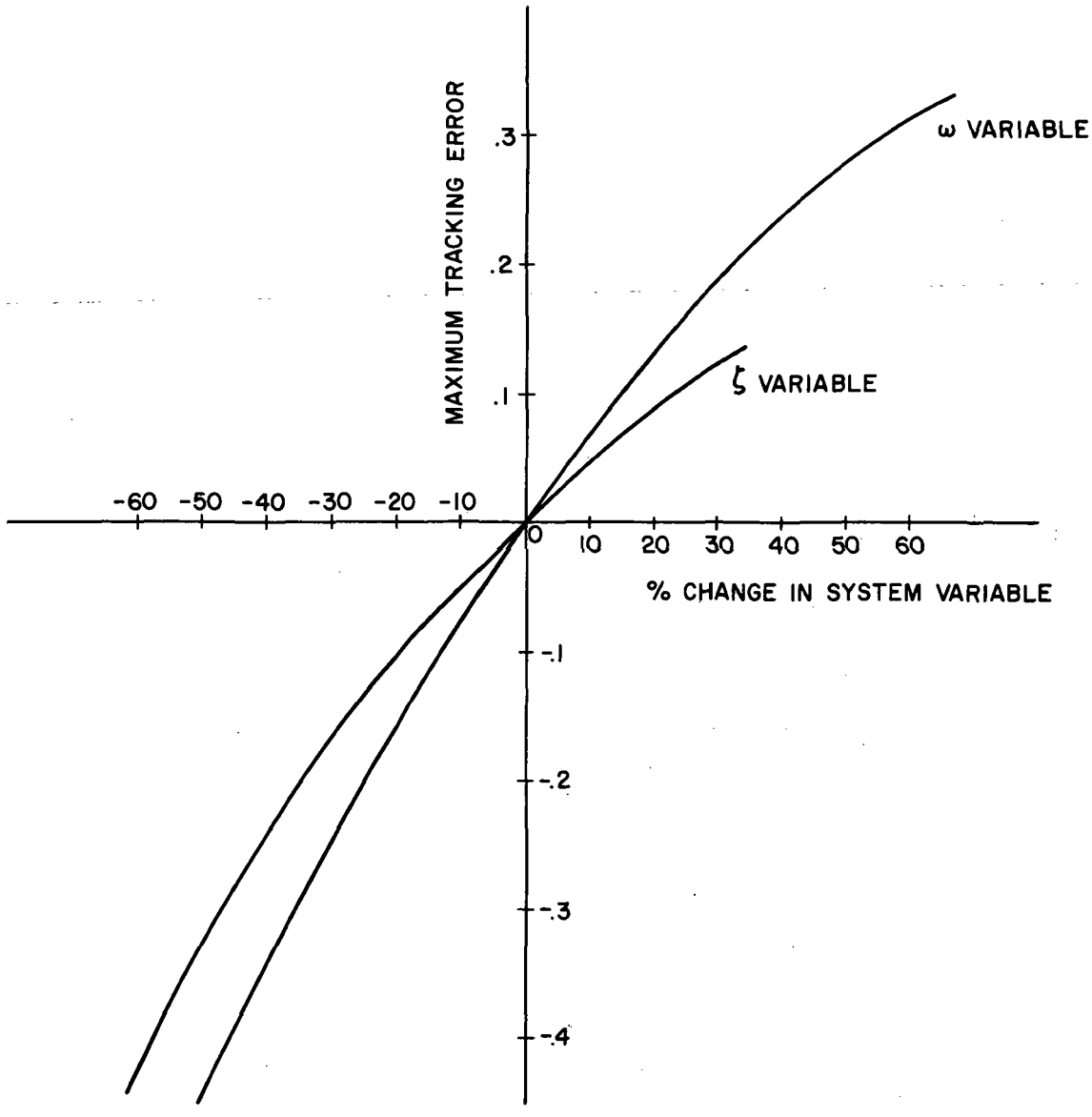

Figure 14. Normalized tracking error vs percentage change in system parameters for second-order systems.

CONCLUSIONS

Two conclusions were formed as a result of this study. First, the inclusion of the external load compensation into the mathematical model improves the reference parameter's tracking accuracy during the presence of

external disturbance to the extent that mathematical modeling is a method of implementing redundancy management for electrohydraulic servoactuators. This technique is being incorporated into a device called the digital interface unit (DIU). The DIU will serve as the junction between a four-line data bus and the servoactuators. In addition to calculating the reference parameter and the tracking error, the DIU will provide the failure detection and correction logic necessary for a fail/operate-fail/operate redundant system. The DIU also converts the actuator position command from a digital to an analog signal and performs a preflight system checkout and inflight status monitoring.

The second conclusion pertains to the choice of a reference parameter. This study has shown the actuator's position to be a better reference parameter than the engine position, which is illustrated by the magnitude of the tracking errors as shown in Figure 9. These differences are the result of using a simplified mathematical model. One can hypothesize that the best reference parameter would be the first measurable state variable; that is, the one which corresponds to the highest order derivative in the system. With a simplified mathematical model, the nonlinearities and higher-order effects which occur after the first measurable parameter produce successively larger tracking errors in the parameters that follow.

APPENDIX

DERIVATION OF SYSTEM EQUATIONS

The equations that are represented in block diagram form in Figure 1 were derived based on the following assumptions:

1. Second-order and nonlinear effects in the servovalve were neglected; the servovalve is represented by a constant K_v, having the units $cm^3/s/deg$.

2. The geometric relationship that describes the linear motion of the actuator as a function of the rotational motion of the engine is

$$X(t) = \theta(t) \quad . \tag{A-1}$$

The ideal actuator position, β_i, can be calculated as

$$\beta_i = \int_0^t \frac{Q(t)}{A} dt \quad , \tag{A-2}$$

where Q (cm^3/s) is servovalve flow rate and A (cm^2) is the piston cross-sectional area.

However, to obtain the actual actuator position, β_a, one must include the effects of the oil compressibility. With the aid of Figure 3 this relationship can be shown to be

$$\beta_a = \beta_i + \frac{K_s}{K_o} (\beta_e - \beta_a) \quad . \tag{A-3}$$

By lumping the structural compliance, K_s, with the oil compliance, K_o, an equivalent spring rate, K_{eq}, can be obtained, where

$$K_{eq} = \frac{K_o K_s}{K_o + K_s} \quad . \tag{A-4}$$

Thus, equation (A-3) can be written as

$$\beta_a = (\beta_i - \beta_e) \frac{K_{eq}}{Ks} + \beta_e \quad . \tag{A-5}$$

The last equation required to describe the system is Euler's equation of motion for the engine. This can be written as

$$K_{eq}(\beta_i - \beta_e) - F_{disturbance} - D\frac{d\beta_e}{dt} = M \frac{d^2\beta}{dt^2} \quad , \tag{A-6}$$

where $F_{disturbance}$ represents the external disturbance force acting on the engine and D is the engine viscous damping coefficient.

A lead-lag pressure feedback compensation network was incorporated into the servovalve to improve its stability and dynamic performance. It is represented in the block diagram as

$$\frac{K_c S}{1 + \tau_f S} \quad .$$

The actuator position was feedback with a gain, K_{fb}, to form the closed-loop system.

APPROVAL

REDUNDANCY MANAGEMENT OF ELECTROHYDRAULIC SERVOACTUATORS BY MATHEMATICAL MODEL REFERENCING

By Richard A. Campbell

The information in this report has been reviewed for security classification. Review of any information concerning Department of Defense or Atomic Energy Commission programs has been made by the MSFC Security Classification Officer. This report, in its entirety, has been determined to be unclassified.

This document has also been reviewed and approved for technical accuracy.

M. A. KALANGE
Chief, Control Mechanisms Branch

C. H. MANDEL
Chief, Guidance and Control Division

F. B. MOORE
Director, Astrionics Laboratory

MSFC—RSA, Ala

DISTRIBUTION

INTERNAL

DIR

DEP-T

AD-S

PD-DIR
Dr. Murphy

PD-DO-DIR
Dr. Thomason

PD-DO-E
Mr. Schultz

S&E-DIR
Mr. Weidner
Mr. Richard

S&E-AERO-DIR
Dr. Geissler
Mr. Horn

S&E-AERO-D
Dr. Lovingood
Dr. Worley

S&E-ASTR-DIR
Mr. Moore
Mr. Horton
Mr. Powell

S&E-ASTR-A
Mr. Hosenthien
Dr. Seltzer
Dr. Borelli
Dr. Clarke
Mr. Kennel
Mr. Carroll
Miss Flowers

S&E-ASTR-G
Mr. Mandel
Dr. Doane
Mr. Wood
Mr. Kelley
Mr. Broussard
Mr. Doran
Mr. Howard
Mr. Jones
Mr. O'Hanian
Mr. Kalange
Mr. Smith
Mr. Cornelius
Mr. Lominick
Mr. Golley
Mr. Krome
Dr. Campbell (15)

S&E-ASTR-C
Mr. Swearingen
Mr. Bridges

S&E-ASTR-I
Mr. Duggen
Mr. Frost

S&E-ASTR-M
Mr. Boehm

S&E-ASTR-S
Mr. Wojtalik
Mr. Scofield
Mr. Justice
Mr. Vallely
Mr. Brooks
Mr. Thompson
Mr. Chubb
Mr. Davis

S&E-CSE-DIR
Dr. Haeussermann

INTERNAL (Concluded)

A&TS-PAT
Mr. L. D. Wofford, Jr.

PM-PR-M

A&TS-MS-H

A&TS-MS-IP (2)

A&TS-MS-IL (8)

A&TS-TU (6)

EXTERNAL

U.S. Army Missile Command
Redstone Arsenal, Ala. 35805
Attn: Mr. Jess Huff, R&E (3)

The Boeing Co.
P. O. Box 39999
Seattle, Wash. 98124
Attn: Mr. C. J. Mason
Mr. Royce Church
Mr. Arthur Boltz
Mr. Bill Walker

McDonnell-Douglas Astronautics Co. (West)
5301 Bolsa Ave.
Huntington Beach, Calif.
Attn: Mr. Chuck Van Ornum (2)

Scientific and Technical Information Facility (2)
P. O. Box 33
College Park, Maryland 20740
Attn: NASA Representative (S-AK/RKT)

Bertea Corp.
18001 Van Karman Ave.
Irvine, Calif. 92664
Attn: Mr. A. P. Henry (2)
Mr. W. D. Wilkerson

Electronic Communications, Inc.
Box 12248
1501 72nd St. N.
St. Petersburg, Fla. 33733
Attn: Mr. Dick Wilkens
Mr. James Kool
Dr. William Marquits

Hydraulic Research
25200 West Rye Canyon Road
Valencia, Calif. 91355
Attn: Mr. Sam Gray (3)

Manned Spacecraft Center
National Aeronautics & Space Administration
Houston, Texas 77058
Attn: Mr. Gene Rice
EG-4, Chief, Systems Development

National Cash Register Co.
16550 W. Bernardo Drive
San Diego, Calif. 92127
Attn: Mr. William Ward
Mr. Russel Gale

Moog, Inc.
Proner Airport
East Aurora, N. Y. 14057
Attn: Mr. Bill Thayer